Zeitschrift für Kristallographie, Bd. 138, S. 274–298 (1973)

High-temperature single-crystal study of the cristobalite inversion*

By **Donald R. Peacor**

Department of Geology and Mineralogy
The University of Michigan[1]

(Received 16 October 1972)

Auszug

Kristalle des Tieftemperatur-Cristobalits von Ellora Caves in Indien wurden mittels Einkristallmethoden bei verschiedenen Temperaturen bis über die Umwandlung in Hochtemperatur-Cristobalit hinaus untersucht. Die Umwandlungstemperatur dieser Kristalle lag um 220 °C. Die Umwandlung verlief träge bei Temperaturen, die bis zu 25 °C von der Gleichgewichtstemperatur abweichen und für die verschiedenen Teile der Kristalle variieren, anscheinend in Abhängigkeit vom Beimengungsgehalt. Die Kristallstruktur der Tieftemperaturform wurde für sieben Temperaturstufen zwischen 28 und 230 °C, die der Hochtemperaturform bei 221, 248, 273 und 310 °C verfeinert. Als Ort des O-Atoms im Hochtemperatur-Cristobalit wurde ein von zwei benachbarten Si-Atomen gleichweit entfernter Kreis mit einem Radius von 0,45 Å gefunden, auf dem das O-Atom statistisch sechs, um $\pi r/3$ aufeinanderfolgende Punkte besetzt. Atomabstände und die Winkel zwischen ihnen sind nahezu gleich denen im Tieftemperatur-Cristobalit. Bei steigender Temperatur bewegen sich die Si- und die O-Atome kontinuierlich auf ihre Lagen im Hochtemperatur-Cristobalit zu.

Abstract

Single crystals of low cristobalite from Ellora Caves, India, were studied using single-crystal x-ray diffraction methods as a function of temperature through the inversion to high cristobalite. The equilibrium inversion temperature in these crystals was approximately 220 °C. The inversion was sluggish with transformations occurring up to 25 °C from the equilibrium temperature, and at varying temperatures for different crystal subvolumes, apparently as a function of variable impurity content. The crystal structure of low cristobalite was refined for data obtained at seven temperatures between 28 and 230 °C, and that of high cristobalite at 221, 248, 273 and 310 °C. The oxygen atom of high

---

* *Dedicated to Professor M. J. Buerger on the occasion of his 70th birthday.* Contribution No. 309, from the Mineralogical Laboratory, Department of Geology and Mineralogy, The University of Michigan.

[1] Ann Arbor, Michigan 48104.

cristobalite was found to be on a circle of radius 0.45 Å, oriented normal to the Si–Si separation. There is one-sixth occupancy of six different equally spaced positions on the circle. Interatomic distances and angles are nearly equivalent to those of low cristobalite. As temperature is increased, both oxygen and silicon atoms of low cristobalite shift continuously and regularly toward the positions finally reached through the inversion to high cristobalite.

Introduction

The characteristics of the inversion of cubic, high cristobalite to tetragonal, low cristobalite have been reviewed by SOSMAN (1965). He notes that the inversion temperature may occur anywhere from 120 to 272 °C, that there is a considerable hysteresis, and that the inversion occurs over a range of temperatures on both heating and cooling. The most probable reasons for these effects are: (1) variable impurity content, (2) differences in particle size, (3) variable degree of structural order. A clear understanding of the nature of the transition depends in large part on an understanding of the crystal-structure relations between the high and low forms. Although the structure of low cristobalite is known in detail, that of high cristobalite is still subject to some question.

The crystal structure of high cristobalite was first investigated by WYCKOFF (1925). Using powder diffraction data from specimens of devitrified glass at 290 and 430 °C, he found that high cristobalite is cubic, $a \sim 7.13$ Å, with space group $Fd3m$. The basic geometry of the crystal structure which he determined has been unaltered by subsequent investigations. It can be viewed as consisting of infinitely extended sheets of SiO_4 tetrahedra, stacked in an *ABC* sequence parallel to [111]. WYCKOFF determined that the bridging O atoms form Si—O—Si angles of 180 °, with Si—O equal to 1.54 Å.

BARTH (1932a) reinvestigated the nature of the high-cristobalite structure using powder data obtained at 500 °C. He observed the presence of several reflections not allowed by space group $Fd3m$, and concluded that the space group is $P2_13$. The structure determined by BARTH has Si—O distances of 1.58 to 1.69 Å and Si—O—Si angles not equal to 180 °.

NIEUWENKAMP (1937) used data from rotating-crystal photographs obtained at 270 °C, and verified WYCKOFF's determination of the space group as $Fd3m$. He found that the best agreement in observed and calculated intensities was obtained with the oxygen atom randomly placed on a circle of radius 0.3 to 0.55 Å, with the plane of the circle bisecting the Si—Si axis.

The low-cristobalite structure was studied by BARTH (1932b) and NIEUWENKAMP (1935). DOLLASE (1965) has refined the structure. Using single crystals from Ellora caves, India, he verified that it has space group $P4_12_1$ or its enantiomorph $P4_32_1$ with $a = 4.97_8$ and $c = 6.94_8$ Å. The crystal structure is a distortional derivative of that of high cristobalite. DOLLASE reported Si—O distances of 1.601 and 1.608 Å and an Si—O—Si angle of 146.8°, in good agreement with values in other tektosilicate structures. The temperature factors (0.83 $Å^2$ and 1.55 $Å^2$ for Si and O, respectively) are unusually high, however. DOLLASE expressed doubt as to be the accuracy of these values, noting, however, that their ratio is consistent with that for Si and O in other well refined structures.

Data on the nature of the high-low transformation have invariably been obtained using powdered material. In order precisely to determine the nature of crystal-structure change as a function of temperature, with special reference to the transformation, this investigation was undertaken with single crystals as studied with a single-crystal diffractometer, and has been carried out in two parts. First, in order to determine the space group of high cristobalite, thermal expansion parameters, and the temperature and rate of transformation, intensities of selected reflections have been studied as a function of temperature and time. Second, three-dimensional intensity data have been obtained, and the crystal structure refined, at seven temperatures for low cristobalite and four temperatures for high cristobalite.

Description of crystals

The crystals used in this study are from the Ellora caves, Hyderabad State, India, and have been described by VAN VALKENBURG and BUIE (1945) and WOLFE (1945). Most of the available crystals were twinned on the spinel law, with obvious reentrant angles. DOLLASE (1965) has described the diffraction relations in the twinned crystals. Several octahedra not having observable reentrant angles were examined using both photographic and diffractometer single-crystal x-ray methods. The twin relations described by DOLLASE (1965) were not found in these crystals, nor was any other evidence of twinning.

Electron microprobe analysis was carried out on two cristobalite crystals and on two paramorphs of quartz after cristobalite. In each case point counts were obtained at several positions in order to test for homogeneity. In addition to Si, analysis was made for Fe, K, Na, Ca and Al. For quartz the averaged weight percents for these elements are 0.01, 0.05, 0.05, 0.10 and 0.15, respectively, while for cristobalite the values are 0.02, 0.03, 0.05, 0.04 and 0.12, respectively. The impurity elements thus amount to less than 0.5% for both the cristobalite and quartz. Furthermore, there are no significant differences between the cristobalite and quartz, nor between different points as selected on individual grains.

Crystals were inserted in silica capillaries and mounted on a Weissenberg-geometry diffractometer fitted with the furnace described by FOIT and PEACOR (1967), such that [111] of the octahedra was the rotation axis. Pulse-height analyzed Mo$K\alpha$ radiation was used throughout this study, with the primary beam monochromated by means of a flat graphite crystal.

Diffraction relations as function of temperature

The first heating experiments were carried out by studying the characteristics of a selected set of reflections as a function of temperature. Several reflections were chosen which would be extinct in the cubic phase, assuming that the unit cell is face-centered. A second set of reflections was selected such that they should be non-extinct for both low and high cristobalite. Two of these were chosen since they are symmetrically non-equivalent in the tetragonal phase, but equivalent in the cubic phase.

Reflections were scanned and graphically recorded, and integrated intensities were determined using a planimeter. Two-theta values were measured for several peaks as the average of two equal-intensity positions on the low and high Υ sides of the peaks. Except near the transformation, all measurements were made only after determining that a steady-state condition had been reached for a given temperature. Both during and after temperature changes a reflection peak intensity was continuously monitored for time periods of up to 12 hours. All intensity variations were found to be time-independent, except while the transformation was occurring.

Figures 1A and 1B show integrated intensity vs. temperature for some selected reflections, the transformation from low to high cristobalite having occurred at 236 ± 5 °C. Immediately following measurements at 236 °C, temperature was increased, such that the intensity of 102 became nearly unobservable within a few seconds with temperature having changed only 1 °C. At 244 °C reflections were scanned. Al

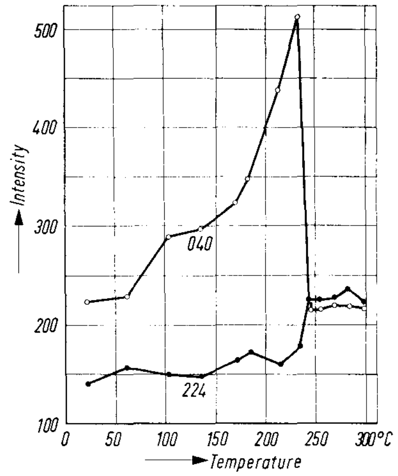

Fig. 1A

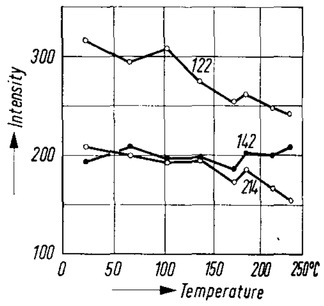

Fig. 1B

Fig. 1A. Intensity as a function of increasing temperature for two reflections (040 and 224) which are not extinct for high cristobalite

Fig. 1B. Intensity as a function of increasing temperature for three reflections (122, 142 and 214) which are extinct for high cristobalite

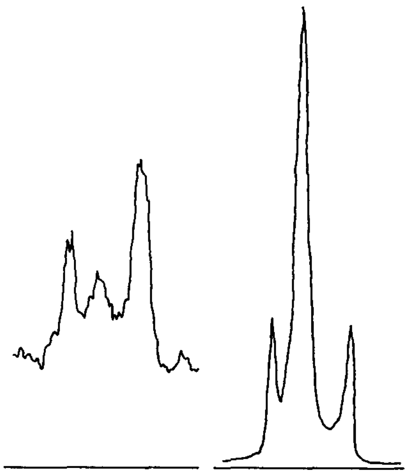

Fig. 2. Scans across the reflection 102. The right-hand scan was obtained at 236 °C with a scale factor of 3000. The left-hand scan was measured at 244 °C with a scale factor of 100

reflections which are extinct for $Fd3m$ were nearly unobservable. At 254 °C all were unobservable.

Figure 2 is a reproduction of the reflection profiles for 102 at 236 °C and 244 °C, with scale factors of 3000 and 100, respectively. The particular crystal being studied was subject to lineage structure which gave rise to the satellites on either side of the main reflections at 236 °C. Aside from the marked decrease in integrated intensity at 244 °C, the principal feature of note is the change in relative intensity for the three domains. At 244 °C the central peak has almost disappeared relative to the two satellites. This shows that the transformation has occurred at different temperatures for different subvolumes of the crystal.

Only a limited number of reflections of each of the two classes of reflections (extinct and non-extinct in high cristobalite) were studied. Nevertheless, the difference in their behavior as a function of temperature was marked enough to allow tentative conclusions to be drawn regarding the nature of change in structure. Most of those reflections which become extinct in high cristobalite exhibit a general, even decline in intensity as a function of increasing temperature, as shown in Fig. 1B. There were marked differences in the behavior of those which are not extinct in high-cristobalite, however. For example, as shown in Fig. 1A, 040 exhibits a continuous increase in intensity, and at 236 °C has an intensity almost double its room-temperature value. The reflections 040 and 224 are symmetrically equivalent in high cristobalite. The ratio $I(040)/I(224)$ exhibits a continuous increase from 0.15 at 28 °C to 0.29 at 236 °C. In addition it increases faster as the transformation is approached. From this limited data, it appears that atomic positional parameters of low cristobalite must be shifting toward those of the high-temperature form as a continuous function of temperature. This tentative conclusion was subsequently verified through refinements of the structure as a function of temperature, as described in a later section.

Observations on the kinetics of inversion

Following the initial inversion to high cristobalite, the crystal was heated to 300 °C with periodic scanning across the selected non-extinct reflections. The crystal was then cooled and heated through the inversion several times in order to study the detailed kinetics. In general, temperature was changed continuously as rapidly as 2 °C/min unless otherwise noted. For these non-steady state conditions, only the intensity of a single reflection was scanned as a function of time and temperature. The sequence of temperature variation, with a description of results, follows:

(1) The crystal was cooled continuously from 300 °C to 192 °C with continuous scanning of 040. No significant change in integrated intensity was noted until the temperature reached 200 °C. At this temperature, the intensity began to decrease continuously, until at 194 °C no further change was observed as a function of either time or temperature.

(2) The temperature was continuously increased to 230 °C, with continuous scanning of 102, which should be extinct in the high-temperature form. From 223 °C to 230 °C the intensity of 102 decreased continuously, becoming unobservable at 230 °C.

(3) The temperature was decreased to 204 °C, with scanning of 102. At 206 °C intensity became observable. The temperature was allowed to drop to 204 °C over a 20 minute interval during which the intensity of 102 continuously increased to a final steady-state value.

(4) The temperature was raised to 228 °C, with scanning of 102. Again at 223 °C, intensity began to decrease continuously. At 228 °C the inversion was nearly complete, but with 102 still observable. That is, both high and low cristobalite coexisted. The crystal was cooled to 215 °C, at which temperature it consisted mostly of high cristobalite.

(5) The temperature was held constant at 215 ± 2 °C for 15 hours. The peak intensity of 102 was continuously monitored. After 15 hours the peak intensity decreased very rapidly to background level. The inversion thus appeared to occur rapidly with temperature held constant. It is possible, however, that the temperature fluctuated one or two degrees. Following complete inversion, the crystal was cooled to room temperature.

These results are consistent with the following relations:

(1) The equilibrium inversion temperature for the crystals studied is slightly less than 220 °C for a large volume of the crystal. The highest temperature of inversion upon cooling was 215 °C, and the lowest upon heating was 223 °C.

(2) There is significant hysteresis in the inversion temperature. The maximum observed for all crystals studied was about 30 °C upon an initial heating sequence. The hysteresis is significantly greater upon the

first heating sequence and decreases with further cycling through the inversion.

(3) The inversion temperature is variable for different portions of the same crystal. A single crystal may show a variation in inversion temperature of up to 10 °C. As a result both low and high cristobalite may coexist near the inversion temperature under constant temperature conditions.

These observations are not unique. SOSMAN (1965) reviewed the nature of similar conclusions regarding the cristobalite inversion, but these studies were all on powdered and mostly synthetic materials where specimen homogeneity was in question. These effects are most readily explained by the presence of impurities, particularly Fe and Al substituting for Si, with Na, K and Ca occupying interframework cavities. The variation in inversion temperature with heating history may likewise be explained by migration of substituting atoms at high temperature. It is also clear that dislocations, perhaps associated with substitutions, may play a primary role in controlling the rate of inversion, particularly relative to diffusion of impurity ions. The observations reported here are only surprising in that the crystals studied have a very low level of impurity elements. This is particularly true with respect to the relatively low value of the transformation temperature, as compared to a value of about 270 °C for synthetic SiO_2.

Twinning relations

Following the first heating-cooling cycle through the inversion, the integrated intensities of all reflections of low cristobalite were markedly reduced relative to their initial values. The inversion to pseudocubic low cristobalite should result in inversion twinning. Scans were therefore made for reflections which would be twin-related to the initial reflections, assuming the twin relation observed by DOLLASE (1965). Peaks at these positions verified that twinning had occurred during the inversion, with three or six different twin domains present. Cooling through a displacive transformation should, theoretically, result in each of the resulting individual domains having equal volume if the crystal is homogeneous in composition and in defects. However, in this case the initial intensities were reduced by a factor of approximately 0.42 rather than 1/3. Further examination of twin-related reflections on this and other crystals confirmed that, although twinning was produced during the inversion, the volumes were not equal. This indicates that the displacements from the higher-symmetry positions do not occur randomly. Local inhomogeneities in substituting atoms could theoretically result in a preference for displacements favoring one domain orientation over another. The inversion in leucite is similar in this regard. Wyart (1938) and Peacor (1968) showed that an originally twinned crystal returned to its initial twinned state following heating and cooling through the inversion. That is, the crystals had a "memory" for the relative volumes of twin domains. Young (1962) has made similar observations on the Dauphiné twinning which occurs with the α-quartz inversion. These relations clearly indicate that the relative twin volumes are controlled by local inhomogeneities.

The presence of untwinned crystals in the rock sample places an upper limit on the temperature of formation. Since cooling through the inversion temperature produces inversion twinning, the untwinned crystals must have formed below the inversion temperature of approximately 220 °C.

Thermal expansion

Figure 3 shows the variation in d as a function of temperature for two of the reflections for which 2θ was measured. Data for these reflections was obtained using different crystals. Least-squares refinement was used to determine precisely these functions. Since the observed values were subject to errors which affected their absolute values, these functions were normalized to the lattice parameters determined by Dollase (1965), to yield the following functions for low cristobalite:

$$a = 4.976\ \text{Å} + 0.973 \times 10^{-4}\ \text{Å} \cdot \mathrm{T}(^\circ\mathrm{C})$$

$$c = 6.940\ \text{Å} + 3.66 \times 10^{-4}\ \text{Å} \cdot \mathrm{T}(^\circ\mathrm{C})\,.$$

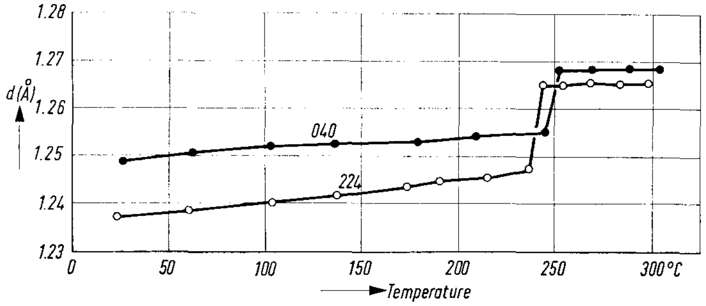

Fig. 3. $d(040)$ and $d(224)$ as a function of temperature

The expansion rate along c is almost four times that along a. A measure of the distortion in the crystal structure of low cristobalite, relative to high cristobalite, can be obtained by comparing the values of $a\sqrt{2}$ and c. The differences between these values (which are identical in high cristobalite) are 0.091 Å at room temperature and 0.046 Å at 220 °C. The difference between these parameters decreases with increasing temperature, apparently reflecting a shift in atom parameters toward those of the cubic phase. The cell edge for high cristobalite at 220 °C is 7.166 ± 0.002 Å. No change in this parameter was detectable over the limited temperature range of these experiments. From the above data, the relative volume change at the transformation is 4.9%.

Structure refinements

Intensity data were obtained for an octahedral crystal measuring approximately 0.25 mm on each edge, and mounted on [111]. The Supper-Pace automated system was used, employing a scan across each reflection with background measured on each side. Mo$K\alpha$ radiation, monochromated with a flat graphite crystal and detected with a scintillation counter, was used. Intensity data were obtained through a single heating sequence at 28, 65, 103, 142, 178, 210 and 230 °C for low cristobalite. The crystal inverted with further temperature increase and the temperature was raised to 310 °C. Data for high cristobalite were then obtained at 310, 273, 248 and 221 °C.

The observed data for low cristobalite consisted of approximately 260 reflections at each temperature. These included 11 reflections which are extinct for space group $P4_12_12$. Approximately 30 reflections were symmetrically related to others, and average values were taken for these. The final sets of data included approximately 216 reflections.

Before measuring data for high cristobalite, the space group was verified as being $Fd3m$ (Wyckoff, 1925; Nieuwenkamp, 1937), as opposed to $P2_13$ (Barth, 1932) by manually scanning over the positions of reflections prohibited by F centering. No reflections were observed. Scans were made for reflections including those reported to be observable on powder photographs by Barth (1932a).

Intensity data for each temperature consisted of 322 observations. These included those required to be extinct for space group $Fd3m$ due to glide planes, and all such intensities were unobservable. From 2 to 12 symmetrical equivalents were measured, and these values were averaged. Each data set then consisted of 59 symmetry non-equivalent intensities.

All data were corrected for Lorentz and polarization effects, including a monochromator polarization factor, but not for absorption ($\mu_1 = 8.2$ cm^{-1}). Unobserved intensities were assigned minimum observable values in accordance with standard counting statistics.

Full-matrix least-squares refinement was carried out for each set of low-cristobalite data under the following conditions. Scattering curves for Si and O were used assuming half ionization. Starting atom parameters were those of DOLLASE (1965) for the room-temperature structure. The weighting scheme of CRUICKSHANK (1965) was used except that all intensities below minimum observable values were rejected. The final R factors, starting with the 28 °C data, are 3.7, 4.3, 4.7, 5.0, 4.7, 5.6 and 5.0%. Refined structure parameters are listed in Table 1. Tables 2 and 3 are listings of structure factors for data measured at 28 and 230 °C, respectively.

For the refinement of the high-cristobalite structure, Si was placed in equipoint $8a$ with coordinates $\frac{1}{8}\frac{1}{8}\frac{1}{8}$, but there was ambiguity in the determination of the oxygen position. NIEUWENKAMP had concluded that oxygen was radially distributed about the Si—Si separation. Ordering of O would require that it be on equipoint $16c$ (000). Refinement of this structure resulted in convergence with $R = 17.5\%$, and isotropic temperature factors of 3.3 and 9.2 for Si and O, respectively. These temperature factors are unreasonably high, even for data measured at 310 °C, and it was concluded that the oxygen atoms were offset from the symmetrical position. Refinements were therefore carried out with oxygen atoms in each of the three equipoints consistent with small shifts from equipoint $16c$. These are: (1) $96h$ ($0x\bar{x}$), (2) $96g$ (xxz), (3) $192i$ (xyz). Refinements for the first two cases resulted in R factors of approximately 6.8%, with atom parameters as listed in Table 4. The refined oxygen positions in each case result in a distribution of six oxygen atoms equally spaced on a circle of radius 0.45 Å. The oxygen atoms of one set are related to the other by a rotation of 30° about the threefold axis, and calculated structure factors are equivalent for both cases.

Refinement was carried out with oxygen in the general position with one twelfth occupancy. The starting position was nearer to that for equipoint $96g$ than to that of $96h$. Following convergence, the R value was 6.0%. Atom parameters are listed in Table 4. The oxygen coordinates are approximately equal to those of equipoint $96g$. Since refinement for all three cases had yielded equivalent results and since there

Table 1. *Refined structure parameters for low cristobalite.* Standard errors in parentheses

		28 °C	65 °C	103 °C	142 °C	179 °C	210 °C	230 °C
Si*	x	0.3002 (1)	0.2990 (1)	0.2988 (2)	0.2977 (1)	0.2966 (2)	0.2952 (2)	0.2943 (2)
	β_{11}	0.0072 (1)	0.0084 (1)	0.0091 (2)	0.0103 (2)	0.0117 (2)	0.0121 (2)	0.0130 (2)
	β_{33}	0.0043 (1)	0.0043 (1)	0.0051 (2)	0.0055 (2)	0.0061 (2)	0.0065 (2)	0.0066 (2)
	β_{12}	0.0002 (2)	0.0002 (3)	0.0001 (3)	— 0.0003 (3)	0.0002 (3)	0.0001 (4)	0.0006 (4)
	β_{13}	0.0004 (1)	0.0008 (1)	0.0008 (2)	0.0008 (1)	0.0013 (2)	0.0011 (2)	0.0013 (2)
O	x	0.2394 (5)	0.2399 (6)	0.2408 (6)	0.2410 (6)	0.2406 (8)	0.2406 (9)	0.2403 (8)
	y	0.1049 (4)	0.1035 (4)	0.1017 (5)	0.0999 (4)	0.0966 (6)	0.0951 (6)	0.0933 (6)
	z	0.1785 (3)	0.1781 (3)	0.1766 (3)	0.1760 (3)	0.1747 (4)	0.1748 (5)	0.1731 (5)
	β_{11}	0.0238 (8)	0.0294 (9)	0.0321 (11)	0.0342 (10)	0.0403 (14)	0.0425 (15)	0.0466 (17)
	β_{22}	0.0068 (5)	0.0080 (5)	0.0113 (6)	0.0117 (6)	0.0141 (7)	0.0124 (8)	0.0145 (7)
	β_{33}	0.0064 (3)	0.0075 (3)	0.0081 (4)	0.0089 (3)	0.0110 (5)	0.0120 (5)	0.0108 (5)
	β_{12}	— 0.0012 (7)	— 0.0006 (8)	— 0.0002 (11)	— 0.0017 (8)	— 0.0011 (11)	0.0002 (11)	— 0.0021 (12)
	β_{13}	0.0026 (4)	0.0037 (5)	0.0034 (6)	0.0047 (6)	0.0057 (9)	0.0044 (10)	0.0053 (10)
	β_{23}	0.0006 (4)	0.0022 (4)	0.0023 (4)	0.0025 (4)	0.0023 (6)	0.0025 (6)	0.0032 (6)

* For Si, $y = x$, $z = 0$, $\beta_{22} = \beta_{11}$, $\beta_{23} = -\beta_{12}$.

were fewer variables for equipoint 96*h*, all subsequent refinements were carried out with oxygen on this equipoint. The final R values are 5.6 (310 °C), 5.4 (273 °C), 5.6 (248 °C) and 6.6% (221 °C). Structure param-

Table 2. *Observed and calculated structure factors for low cristobalite,* 28 °C

h	k	l	F_o	F_c
0	0	4	89.0	89.8
		8	25.3	26.2
0	1	2	93.4	90.7
		3	10.7	13.0
		4	37.0	36.9
		5	94.3	94.4
		6	3.2	2.2
		7	41.0	42.3
		8	3.3	5.9
		9	17.1	17.3
		10	11.0	10.8
0	2	0	168.8	165.0
		2	66.8	62.0
		3	83.0	81.4
		4	76.6	77.3
		5	28.2	29.2
		6	13.8	13.4
		7	42.2	41.1
		8	34.2	34.4
		9	35.7	34.9
		10	13.7	14.6
0	3	2	102.5	103.2
		3	55.4	55.7
		4	9.0	7.7
		5	10.8	9.3
		6	45.5	44.3
		7	3.3	0.3
		8	3.6	0.2
		9	3.7	6.8
		10	27.8	27.8
0	4	0	25.8	23.3
		1	80.6	81.9
		2	44.7	43.7
		3	54.0	52.6
		4	25.1	24.5
		5	41.7	41.9
		6	13.1	13.9
		7	27.5	26.1
		8	15.7	15.1
		9	19.9	20.7
		10	16.8	17.8
0	5	2	61.3	59.0
0	5	3	3.3	4.1
		4	24.5	26.0
		5	3.4	2.1
		6	60.8	61.8
		7	8.9	7.7
		8	10.0	8.6
		9	3.8	8.6
0	6	0	9.7	7.4
		2	3.5	3.9
		3	32.8	31.8
		4	20.9	20.6
		5	28.4	28.5
		6	8.2	1.3
		7	15.7	13.1
		8	23.4	22.3
0	7	2	38.0	37.6
		3	34.6	34.0
		4	3.6	0.9
		5	3.6	0.2
		6	20.3	21.2
0	8	0	16.8	15.6
		2	3.7	2.9
		3	18.3	20.7
1	1	3	99.2	97.2
		4	8.7	7.8
		5	11.3	12.0
		6	104.4	106.6
		7	3.3	2.5
		8	3.3	4.5
1	2	0	6.0	4.0
		1	44.6	44.8
		2	73.7	72.2
		3	41.9	42.8
		4	72.6	73.1
		5	67.7	68.0
		6	12.0	11.9
		7	48.0	48.9
		8	47.5	47.6
1	3	0	36.8	36.3
		1	67.8	66.8
		2	68.7	69.0
		3	74.9	76.7
1	3	4	50.7	51.3
		5	36.0	34.5
		6	28.8	30.0
		7	27.5	27.6
		8	15.4	14.3
1	4	0	95.4	96.2
		1	30.1	29.4
		2	23.9	25.6
		3	23.5	23.1
		4	68.2	68.6
		5	25.8	25.8
		6	5.7	5.0
		7	28.3	27.5
		8	35.4	34.6
1	5	0	26.2	25.9
		1	37.9	37.5
		2	6.0	6.5
		3	30.0	28.9
		4	21.7	21.8
		5	56.9	57.7
		6	6.8	3.5
		7	39.7	40.1
		8	8.8	10.5
1	6	0	66.2	65.3
		1	16.0	15.7
		2	16.7	14.0
		3	25.5	26.1
		4	44.9	43.3
		5	8.1	7.8
		6	11.9	11.2
		7	15.9	12.8
1	7	0	14.9	13.5
		1	21.7	22.6
		2	37.2	37.2
		3	22.9	24.8
		4	14.3	13.1
		5	17.4	19.2
		6	10.9	3.7
1	8	0	3.7	4.8
		1	12.6	13.2
		2	3.9	9.5
		3	21.8	22.9
2	2	0	47.2	48.5
		1	16.4	14.7
		2	32.1	32.0
		3	77.9	77.7
		4	64.7	65.1
		5	35.9	34.9
		6	30.7	31.9
2	3	0	3.2	3.7
		1	50.3	50.8
		2	76.7	77.7
		3	64.4	65.0
		4	32.0	33.5
		5	29.7	29.4
		6	38.6	37.1
2	4	0	11.3	12.1
		1	59.0	60.7
		2	45.0	45.6
		3	40.2	38.6
		4	21.6	23.6
		5	34.7	36.3
		6	36.2	34.8
2	5	0	14.2	15.0
		1	24.0	24.6
		2	39.8	41.1
		3	25.4	25.0
		4	17.9	18.0
		5	27.2	27.1
		6	51.6	51.9
2	6	0	3.5	3.4
		1	44.0	45.4
		2	31.6	31.1
		3	21.8	20.1
		4	17.8	14.8
		5	25.9	26.3
		6	23.1	23.1
2	7	0	23.7	23.4
		1	24.5	24.6
		2	28.5	27.1
		3	26.6	26.2
		4	11.9	11.0
		5	13.8	13.8
2	8	0	15.3	15.1
2	8	1	11.9	14.1
		2	10.7	10.6
3	3	0	64.6	65.1
		1	55.0	54.8
		2	58.9	61.3
		3	43.6	44.6
		4	46.3	46.5
3	4	0	56.5	59.2
		1	44.1	44.3
		2	20.0	21.0
		3	49.4	49.3
		4	31.1	31.8
3	5	0	48.8	49.2
		1	24.4	23.6
		2	11.8	11.1
		3	3.5	6.4
		4	44.2	43.9
3	6	0	42.8	42.7
		1	28.5	30.0
		2	10.5	10.7
		3	25.5	25.7
		4	18.5	19.8
3	7	0	26.5	26.0
		1	21.5	21.6
		2	18.2	17.1
		3	13.8	13.7
		4	23.8	25.9
4	4	0	23.4	24.7
		1	28.2	28.3
		2	57.0	57.8
4	5	0	3.5	7.2
		1	33.2	33.9
		2	3.7	5.8
4	6	0	6.8	2.3
		1	17.4	16.9
		2	40.4	41.2
4	7	0	20.3	19.2
		1	23.6	21.7
		2	8.0	8.7
5	5	0	38.8	37.3
5	6	0	9.0	7.8

Table 3. *Observed and calculated structure factors for low cristobalite,* 230 °C

h	k	l	F_o	F_c
0	0	4	68.5	70.5
		8	31.5	29.3
0	1	2	77.4	76.7
		3	13.3	14.4
		4	33.4	32.8
		5	75.0	76.2
		6	3.2	1.3
		7	40.2	40.6
		8	7.9	7.3
		9	16.4	15.4
		10	9.8	10.1
0	2	0	146.4	144.4
		1	19.9	16.1
		2	69.1	63.6
		3	70.5	69.7
		4	73.1	73.6
		5	27.5	26.6
		6	3.1	4.5
		7	29.4	28.1
		8	31.2	32.7
		9	19.7	22.6
		10	14.1	9.9
0	3	1	96.7	95.1
		2	76.5	78.7
		3	54.1	54.1
		4	3.2	1.6
		5	9.5	7.9
		6	38.9	37.5
		7	8.0	6.2
		8	3.5	0.8
		9	10.6	11.2
		10	19.2	19.1
0	4	0	34.6	32.4
		1	72.7	73.2
		2	28.4	29.4
		3	36.0	35.4
		4	29.8	28.0
		5	30.3	30.1
		6	6.1	4.2
		7	19.1	20.8
		8	16.4	15.6
		9	15.2	13.7
		10	3.8	10.0
0	5	1	15.8	15.8
0	5	2	47.3	47.3
		3	3.3	1.3
		4	19.1	17.5
		5	6.8	6.3
		6	44.5	46.7
		7	3.7	5.7
		8	8.8	6.4
		9	3.7	4.2
0	6	0	14.7	15.1
		1	37.6	37.9
		2	12.1	9.2
		3	27.3	27.4
		4	9.0	9.7
		5	24.5	23.6
		6	6.7	2.8
		7	13.1	12.3
		8	3.8	8.3
0	7	1	10.2	9.8
		2	33.0	31.9
		3	15.6	15.2
		4	7.3	4.6
		5	3.6	0.4
		6	13.4	14.1
0	8	0	15.2	12.7
		1	3.8	4.4
		2	3.7	0.6
		3	14.8	15.9
1	1	3	83.1	82.7
		4	6.3	3.3
		5	13.2	11.1
		6	88.6	90.2
		7	3.2	3.2
		8	3.3	4.0
1	2	0	6.2	4.4
		1	36.7	38.6
		2	64.0	62.4
		3	52.8	51.0
		4	63.3	62.8
		5	60.4	61.1
		6	7.0	7.9
		7	39.6	40.3
		8	31.4	32.0
1	3	0	25.7	26.3
		1	54.2	54.5
1	3	2	72.1	71.2
		3	55.4	57.1
		4	38.2	39.4
		5	33.6	32.8
		6	27.6	27.3
		7	19.5	21.0
		8	10.6	11.4
1	4	0	86.4	87.2
		1	18.6	17.3
		2	23.9	24.6
		3	24.5	23.8
		4	50.8	50.4
		5	24.0	24.3
		6	3.3	1.2
		7	19.7	20.1
		8	24.0	24.2
1	5	0	17.1	17.7
		1	32.6	32.7
		2	3.3	6.2
		3	25.3	24.1
		4	11.3	12.9
		5	42.8	43.4
		6	12.5	11.8
		7	25.8	27.9
		8	3.7	8.1
1	6	0	48.0	47.6
		1	13.4	14.0
		2	3.4	5.2
		3	17.4	15.8
		4	36.3	35.4
		5	3.7	4.4
		6	3.7	4.5
		7	10.2	7.3
		8	16.0	16.2
1	7	0	7.1	9.1
		1	20.5	20.6
		2	16.3	17.2
		3	20.5	22.6
		4	8.5	7.3
		5	12.4	10.4
		6	3.7	1.2
1	8	0	10.3	8.0
		1	11.3	9.9
		2	3.7	6.4
1	8	3	8.8	9.0
2	2	0	38.3	40.0
		1	11.3	9.8
		2	25.0	24.9
		3	68.2	67.9
		4	67.8	67.9
		5	31.3	31.2
		6	20.7	21.9
2	3	0	9.8	9.3
		1	42.8	42.8
		2	60.9	61.8
		3	60.1	60.5
		4	27.3	27.7
		5	20.9	21.1
		6	31.1	31.8
2	4	0	10.4	3.5
		1	52.9	54.2
		2	33.7	32.2
		3	32.5	30.9
		4	27.5	26.5
		5	25.6	26.3
		6	22.3	22.2
2	5	0	3.2	2.9
		1	18.0	18.0
		2	35.0	35.5
		3	18.8	19.7
		4	11.5	14.1
		5	16.1	18.9
		6	37.4	38.3
2	6	0	7.3	6.3
		1	29.4	29.4
		2	23.5	24.0
		3	19.4	20.4
		4	7.4	6.6
		5	20.3	19.5
		6	13.6	14.5
2	7	0	11.6	9.1
		1	14.9	14.7
		2	25.0	24.5
		3	13.4	13.2
		4	3.7	5.5
		5	3.8	8.2
2	8	0	13.9	11.2
		1	6.7	6.2
2	8	2	9.8	7.8
3	3	0	44.5	45.4
		1	44.5	46.0
		2	55.5	55.1
		3	32.4	31.9
		4	32.2	32.4
3	4	0	51.7	53.0
		1	32.0	31.0
		2	20.4	20.9
		3	34.4	36.3
		4	25.5	23.9
3	5	0	34.0	34.1
		1	21.5	21.7
		2	9.0	9.1
		3	10.4	9.7
		4	30.6	30.9
3	6	0	29.9	29.3
		1	19.2	21.1
		2	3.6	2.0
		3	21.4	18.2
		4	18.7	18.5
3	7	0	19.4	18.6
		1	12.0	14.6
		2	8.2	8.7
		3	11.7	12.5
		4	14.2	15.0
4	4	0	8.1	5.4
		1	25.8	29.4
		2	39.0	39.7
4	5	0	9.1	11.2
		1	22.2	23.1
		2	10.2	11.6
4	6	0	3.7	2.4
		1	9.6	11.0
		2	27.2	27.3
4	7	0	8.9	7.4
		1	13.5	14.3
		2	9.9	9.8
5	5	0	27.2	27.4
5	6	0	7.3	5.7

eters are listed in Table 5. Table 6 contains a listing of the structure factors for the 310 °C data.

Interatomic distances and angles are listed in Tables 7 and 8 for low and high cristobalite, respectively. These were calculated with no correction for thermal motion, but the lattice parameters were adjusted to account for thermal expansion. Standard errors were calculated using the least-squares variance-covariance matrix and lattice-parameter standard errors.

Table 4. *Refined oxygen-atom parameters for high cristobalite with oxygen on four different equipoints*

Equipoint	16c	96g	96h	192i
x	0	0.0257	0.0439	0.024
$\sigma(x)$		(0.0019)	(0.0006)	(0.012)
y		0.0257	— 0.0439	0.026
$\sigma(y)$				(0.009)
z		— 0.0501		— 0.030
$\sigma(z)$		(0.0020)		(0.003)
B	9.2	3.7	3.6	3.9 Å^2
$\sigma(B)$		(0.2)	(0.2)	(0.2)

Table 5. *Refined structure parameters for high cristobalite*
Standard errors in parentheses

		221 °C	248 °C	273 °C	310 °C
Si[1]	β_{11}	0.0162 (2)	0.0160 (2)	0.0165 (1)	0.0162 (2)
O[2]	y	0.0444 (11)	0.0435 (8)	0.0440 (7)	0.0427 (9)
	β_{11}	0.0147 (27)	0.0166 (22)	0.0169 (19)	0.0192 (26)
	β_{22}	0.0181 (14)	0.0179 (9)	0.0195 (9)	0.0190 (10)
	β_{12}	0.0013 (15)	−0.0005 (13)	0.0002 (10)	−0.0002 (14)
	β_{23}	−0.0011 (22)	0.0013 (16)	−0.0016 (15)	0.0001 (17)

[1] For Si, $x = y = z = 1/8$; $\beta_{11} = \beta_{22} = \beta_{33}$; $\beta_{12} = \beta_{13} = \beta_{23} = 0$.

[2] For O, $x = 0$; $z = -y$; $\beta_{33} = \beta_{22}$; $\beta_{13} = \beta_{12}$.

Table 6. *Observed and calculated structure factors for high cristobalite,* 310 °C

h	k	l	F_o	F_c	h	k	l	F_o	F_c	h	k	l	F_o	F_c	h	k	l	F_o	F_c	h	k	l	F_o	F_c
2	2	0	104.3	-103.8	3	3	5	23.3	-23.6	1	3	7	21.7	-22.4	4	4	8	11.3	12.6	1	7	9	4.6	4.3
2	2	2	84.0	80.1	1	5	5	21.7	-22.7	3			13.6	-13.5	2	6	8	12.7	12.2	3			4.6	- 3.7
1	1	3	23.6	-24.7	3			19.1	-19.3	1	5	7	14.5	-13.6	4			4.5	1.2	0	2	10	11.3	-10.6
1	3	3	80.9	80.4	5			19.3	20.9	3			12.8	14.2	0	8	8	4.8	5.6	2			4.5	- 1.6
3			51.1	49.1	0	2	6	54.6	54.9	5			10.8	9.8	2			4.5	0.8	2	4	10	9.3	8.2
0	0	4	32.0	-32.4	2			7.2	6.7	1	7	7	5.6	7.7	4			4.8	- 4.9	4			4.6	0.9
4			75.5	77.6	2	4	6	29.2	-30.0	3			9.5	10.0	1	1	9	10.8	-11.1	0	6	10	4.7	6.0
2	2	4	79.5	78.6	4			4.1	4.0	5			4.5	- 4.5	1	3	9	11.6	-10.7	2			4.6	- 0.7
2	4	4	10.5	10.0	0	6	6	18.8	-18.5	0	0	8	26.8	27.3	3			10.3	8.7	1	3	11	4.6	3.8
4			35.9	-34.4	2			4.3	- 0.2	2	2	8	23.0	-21.8	1	5	9	8.7	9.1	3			4.6	4.5
1	1	5	40.8	40.9	4			17.7	19.1	0	4	8	20.3	-20.5	3			7.8	6.2	1	5	11	4.6	2.7
1	3	5	49.7	50.6	1	1	7	29.1	29.8	2			4.3	2.5	5			4.5	- 2.9					

Table 7. *Interatomic distances and angles, and equivalent isotropic temperature factors for low cristobalite*

Standard errors in parentheses

	28 °C	65 °C	103 °C	142 °C	179 °C	210 °C	230 °C
Si—O	1.605 (2)	1.604 (2)	1.603 (2)	1.602 (2)	1.604 (3)	1.606 (3)	1.600 (3) Å
Si—O^1	1.613 (2)	1.609 (2)	1.607 (2)	1.606 (2)	1.599 (3)	1.599 (3)	1.599 (3)
O—O^{11}	2.656 (4)	2.660 (4)	2.653 (5)	2.655 (5)	2.650 (6)	2.660 (7)	2.645 (7) Å
O—O^1	2.633 (3)	2.631 (3)	2.626 (3)	2.625 (3)	2.624 (4)	2.624 (5)	2.625 (4)
O—O^{111}	2.600 (1)	2.601 (2)	2.597 (2)	2.596 (2)	2.593 (2)	2.596 (2)	2.591 (2)
O^1—O^{111}	2.620 (4)	2.618 (5)	2.623 (5)	2.619 (5)	2.604 (6)	2.596 (7)	2.596 (7)
O—Si—O^{11}	111.7 (2)	112.0 (2)	111.7 (2)	111.9 (2)	111.4 (3)	111.8 (3)	111.5 (3) Å
O—Si—O^1	110.0 (1)	109.9 (2)	109.8 (2)	109.8 (2)	110.0 (2)	110.0 (3)	110.2 (3)
O—Si—O^{111}	108.0 (1)	108.1 (1)	108.0 (1)	108.0 (1)	108.1 (1)	108.2 (1)	108.2 (1)
O^1—Si—O^{111}	109.1 (2)	108.9 (2)	109.4 (2)	109.2 (2)	109.1 (3)	108.6 (3)	108.5 (3)
Si—O—Si^1	146.4 (1)	146.6 (2)	147.5 (2)	147.9 (2)	148.8 (2)	148.7 (2)	149.4 (2)
$B_{\text{equiv.}}$ (Si)	0.76	0.83	0.93	1.04	1.17	1.22	1.29 Å^2
$B_{\text{equiv.}}$ (O)	1.43	1.72	1.96	2.10	2.51	2.59	2.65

Table 8. *Structure parameters for high cristobalite*

	221 °C	248 °C	273 °C	310 °C
Si–O	1.615 (3)	1.613 (2)	1.614 (2)	1.611 (2) Å
Si–O–Si	147.7 °	148.3 °	148.0 °	148.9 °
$B_{equiv.}$ (Si)	3.33	3.29	3.39	3.33 Å^2
$B_{equiv.}$ (O)	3.51	3.59	3.83	3.92

High-cristobalite structure

As described above, the results of the refinement are consistent with NIEUWENKAMP's conclusion (1937) that the oxygen atom is radially distributed about the Si—Si separation. The Si—O distances (1.611—1.615 Å) and the Si—O—Si angles (148.9—147.7 °) are consistent with values in other well refined tektosilicates. The radius of the circle on which the six oxygen atoms are distributed is constant within standard error, varying only between 0.44 and 0.45 Å for the four refinements.

These results are unfortunately still ambiguous relative to the position of oxygen. The x-ray diffraction data are consistent with either of several interpretations: (1) Oxygen, when placed in the general position, refined to the special position. This equipoint requires one sixth occupancy of each of six positions, separated by rotations of 60 °, on a circle about the Si—Si separation. Thus the oxygen atom appears, on the average, to prefer these positions as opposed to a general, random position on the circle. (2) A given oxygen atom might occupy only one of these positions with no change with time, such that all six positions are equally but randomly occupied over the entire crystal. (3) Each oxygen atom may be shifting from one position to another, occupying only one position one sixth of the time. The x-ray results do not unambiguously allow a choice to be made between the latter two possibilities. However, interatomic distances and angles do provide some evidence. There are 24 oxygen positions (four sets of six) for each tetrahedron, and O—O distances and O—Si—O angles were computed for these. Combinations of four were examined relative to reasonable distance and angle values expected for tetrahedron geometry. Only one set of four gives reasonable values. For this set there are four O—O distances of 2.606 Å and two of 2.677 Å, with four angles of 108.0 ° and two of 112.4 °. These values are very close to those determined for low cristobalite. There are six such symmetrically equivalent sets and among them all 24 oxygen positions around a given Si are accounted

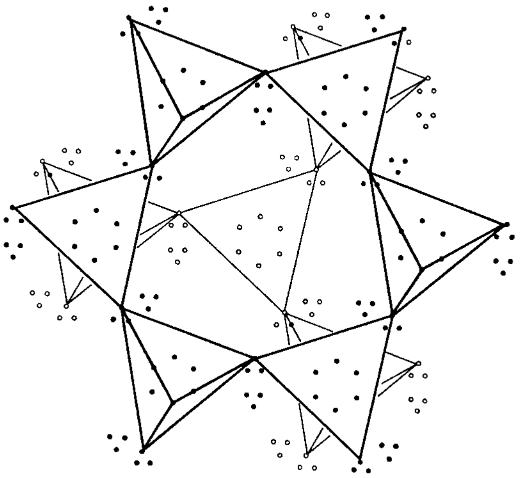

Fig. 4. A portion of the structure of high cristobalite projected on (111). Parts of two layers of tetrahedra are shown

for. Figure 4 is a diagram of a portion of the high-cristobalite structure projected down [111], with tetrahedra outlined for one of the six symmetrical sets of oxygen atoms. One interpretation of the structure of a cristobalite crystal, then, is that it consists of domains of each of the six orientations of oxygen atoms, either in static or, more probably, dynamically changing configurations. This interpretation is a sufficient but not necessary one, and until data of other kinds are available, must be regarded as problematical at best.

Low-cristobalite structure

The room-temperature structure parameters are equivalent to those obtained by DOLLASE (1965) and will not be further discussed here. Of prime interest, however, is the nature of the change in structure parameters as a function of temperature. Figures 5—8 are plots of such functions. Interatomic distances are simply the distances between mean atom position, uncorrected for thermal motion.

The coordinates of both silicon and oxygen change regularly as a function of temperature. The oxygen and silicon atoms shift 0.07 and 0.04 Å, respectively, from 28 to 230 °C. Of greater interest are the directions of shift. The shift vector for oxygen has fractional coordinates 0.0010, —0.0112, —0.0053. The vector from the oxygen position at 28 °C to that of the position attained in the cubic structure (the

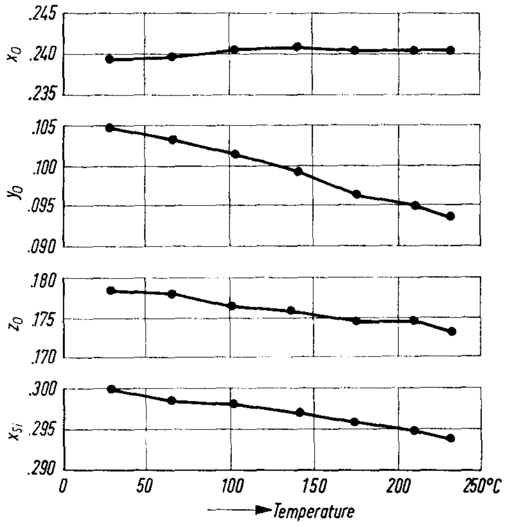

Fig. 5. Coordinates of Si and O atoms as a function of temperature for low cristobalite

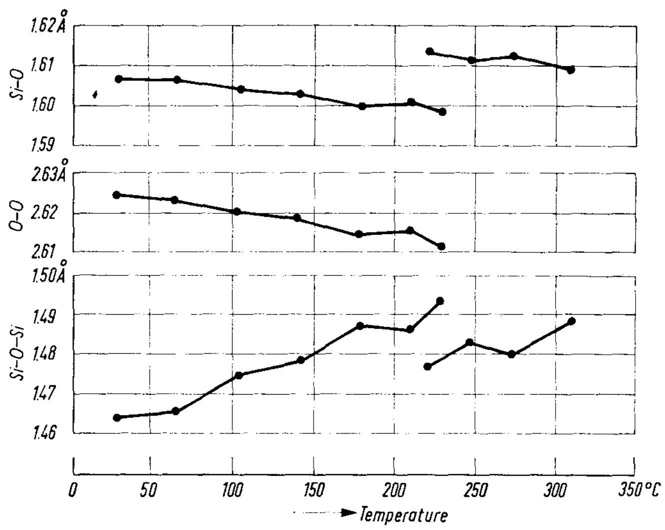

Fig. 6. Si—O—Si angle, O—O distance and Si—O distance as a function of temperature. The O—O and Si—O distances are averages for the low-cristobalite structure

Table 9. *Magnitudes of the principal axes of the thermal ellipsoids of low cristobali*
Standard errors in parentheses

Atom	Axis	28 °C	65 °C	103 °C	142 °C	178 °C	210 °C	230°C
Si	r_1	0.092 (2)	0.092 (2)	0.099 (2)	0.107 (2)	0.108 (3)	0.114 (3)	0.115 (3)
	r_2	0.097 (2)	0.104 (2)	0.108 (2)	0.112 (2)	0.123 (2)	0.124 (2)	0.128 (2)
	r_3	0.105 (2)	0.112 (2)	0.118 (2)	0.125 (2)	0.134 (2)	0.136 (3)	0.141 (2)
O	r_1	0.091 (4)	0.091 (4)	0.109 (4)	0.107 (4)	0.125 (4)	0.120 (4)	0.121 (4)
	r_2	0.121 (3)	0.135 (3)	0.144 (4)	0.150 (3)	0.161 (4)	0.170 (4)	0.167 (4)
	r_3	0.177 (3)	0.197 (3)	0.205 (4)	0.215 (3)	0.234 (4)	0.237 (5)	0.243 (5)

oxygen position is taken at the symmetrical site 000 along the Si–Si separation), has coordinates 0.0106, —0.1049, —0.0535. The oxygen shift vector, when multiplied by a factor of 10 is equal, within standard error, to the difference between the oxygen positions at 28 °C and in the cubic structure. Thus the oxygen atom moves continuously, and regularly from its position at 28 °C toward that of the cubic structure. The shift is approximately $10\,^0/_0$ of the total separation between the oxygen atom at 28 °C and that of high cristobalite. The silicon atom shifts in a similar way. The shift vector in low cristobalite from 28 °C to 230 °C is —0.0057, —0.0057, 0.0, while the difference in coordinates between silicon in the 28 °C structure and that of high cristobalite is —0.0501, —0.0501, 0.0. These relations are graphically illustrated in Fig. 9.

The relative orientations of the principal axes of vibration of the oxygen ellipsoid (Table 10) show little variation as a function of temperature. In addition, the relative magnitudes (Table 9) and orientations of these axes are similar to those of other silicates; that is, r_3 is approximately normal to the Si—O—Si plane, while r_1 is approximately parallel to the Si—Si separation. The orientation of the principal axis r_3 is nearly constant over all temperatures, while the changes in r_1 and r_2 correspond only to limited rotation of these two axes (up to 20°) about r_3.

The magnitudes of the principal axes of vibration of both Si and O (Fig. 7) increase fairly regularly. As we have found for a number of other structures, the increases are approximately linear, within standard error, with slopes proportional to room-temperature values of the temperature factors. The equations of the equivalent isotropic temperature factors as a function of temperature (Fig. 8) were determined by least-squares, and found to extrapolate to —213 °C and —252 °C for oxygen and silicon, respectively, for $B = 0$. The temperature factor

Table 10. *Orientations of the principal axes of the thermal ellipsoids of low cristobalite.* Standard error in parentheses

Atom	Ellipsoid axes	Crystal axes	28 °C	65 °C	103 °C	142 °C	178 °C	210 °C	230 °C
Si	r_1	a_1	129 (3)°	122 (2)°	125 (2)°	121 (2)°	121 (2)°	123 (2)°	120 (2)°
		a_2	51 (3)	58 (2)	55 (2)	59 (2)	59 (2)	57 (2)	60 (2)
		c	64 (6)	48 (4)	54 (5)	47 (4)	47 (3)	50 (4)	45 (4)
	r_2	a_1	135	135	135	135	135	135	135
		a_2	135	135	135	135	135	135	135
		c	90	90	90	90	90	90	90
	r_3	a_1	72 (4)	62 (2)	65 (3)	61 (3)	61 (2)	63 (3)	60 (2)
		a_2	108 (4)	118 (2)	115 (3)	119 (3)	119 (2)	117 (3)	120 (2)
		c	26 (6)	42 (4)	36 (5)	43 (4)	43 (3)	40 (4)	45 (4)
O	r_1	a_1	84 (3)	84 (2)	83 (3)	79 (2)	81 (3)	87 (2)	81 (2)
		a_2	14 (5)	26 (3)	31 (4)	33 (3)	28 (4)	17 (4)	30 (4)
		c	102 (5)	115 (3)	120 (4)	120 (3)	116 (5)	107 (4)	119 (4)
	r_2	a_1	75 (2)	73 (2)	76 (3)	75 (2)	72 (3)	73 (3)	76 (3)
		a_2	104 (5)	116 (3)	121 (4)	123 (3)	118 (5)	107 (4)	120 (4)
		c	160 (4)	149 (3)	145 (4)	143 (3)	146 (5)	155 (4)	146 (4)
	r_3	a_1	16 (2)	18 (2)	16 (3)	19 (2)	20 (3)	17 (3)	16 (3)
		a_2	93 (2)	89 (2)	88 (3)	91 (2)	90 (2)	88 (2)	91 (2)
		c	74 (2)	72 (2)	74 (2)	71 (2)	70 (3)	73 (3)	74 (3)

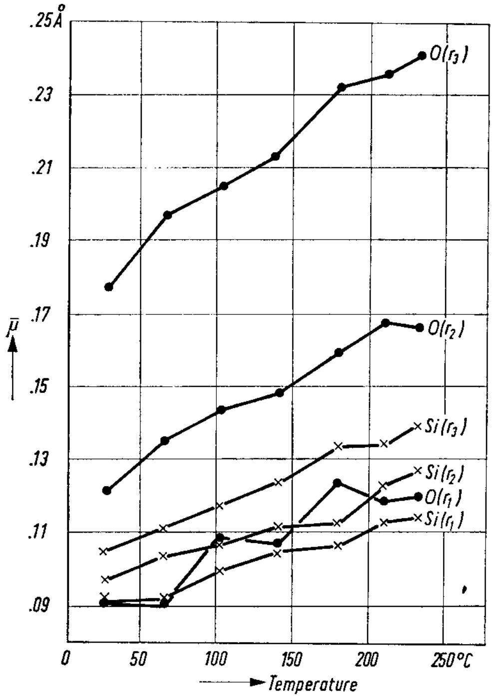

Fig. 7. Magnitudes of the principal axes of vibration of Si and O as a function of temperature

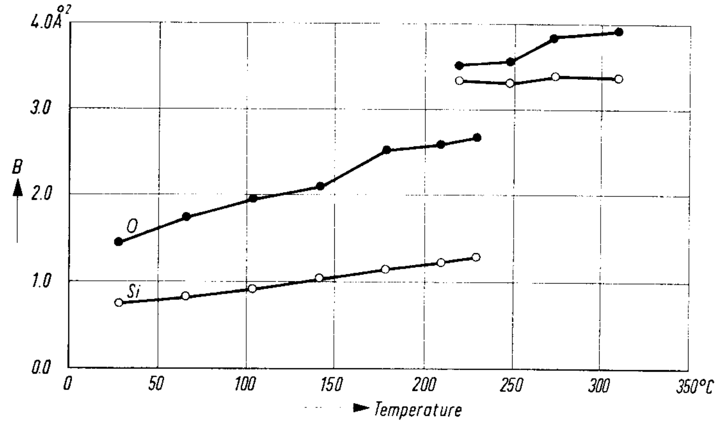

Fig. 8. Equivalent isotropic temperature factors as a function of temperature

reflects both thermal vibration and positional disorder. If the latter factor is significant the temperature factors should be positive at 0 °K. This was the case, for example, with the nepheline structure as a func-

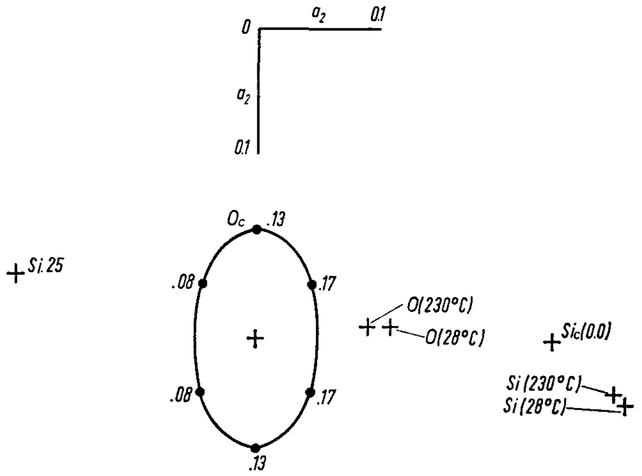

Fig. 9. Projection down [010] of low cristobalite of two Si atoms and a bridging O atom. The positions of a Si and an O atom at 28 and 230 °C are shown, as well as the positions of O and Si in high cristobalite (labelled with subscript c)

tion of temperature (Foreman and Peacor, 1970), where positional disorder was known to exist. The temperature factor values for low cristobalite thus appear to reflect a lack of significant positional disorder. This conclusion is also supported by the data on orientations of the principal axes of oxygen. The values are similar to those of other silicates where positional disorder is lacking. The exceptionally high room-temperature values for both Si and O as reported both by Dollase (1965) and in this paper appear to be real.

The magnitudes of the principal axes of the thermal-vibration ellipsoid are proportional to the bonding-force constants in those directions. Thus the principal axis r_3 of oxygen is oriented approximately normal to the Si—O—Si bonding plane at all temperatures for low cristobalite. Accordingly, the potential-energy minimum occupied by oxygen is at a point such that the potential rises relatively rapidly in directions approximately normal to r_3. The oxygen atom shifts in a direction approximately 94° from r_3, however, in a direction of relatively rapidly varying potential energy. The shift of the oxygen atom, then, must not be due to anharmonic vibration, but in response to a regular change in the form of the potential well, and thus to a change in the character of bonding of Si and O. This is reflected in the changes in the Si—O distance and the Si—O—Si angle (Fig. 6). These values change fairly regularly and approximately linearly as a function of temperature. The Si—O interatomic distance decreases slightly with increasing temperature. Similar behavior has been noted for other structures with increasing temperature. For example, YOUNG (1962) reports a decrease in the Si—O distance from 1.607 Å at 23 °C to 1.598 Å at 570 °C in α quartz. The decrease is probably only apparent, however, as these distances are calculated without a thermal correction. Such a correction cannot be made accurately at this time and even if it were, would not include corrections for anharmonic vibration. The apparent decrease in Si—O is accompanied by an increase in the Si—O—Si angle. At the inversion temperature these trends are reversed, the transformation to high cristobalite being characterized by a marked increase in Si—O and a decrease in Si—O—Si. The accuracy of the absolute values notwithstanding, it is clear that these two parameters are closely coupled, and that their changes at the transformation reflect a significant change in the character of the Si—O bond.

Thermal expansion

High cristobalite has the extremely low value of linear coefficient of thermal expansion of 2.08×10^{-5} Å/°C (JOHNSON and ANDREWS, 1956), as qualitatively verified by the data of Fig. 3. In contrast, low cristobalite has expansion coefficients of 9.27×10^{-5} and 3.51×10^{-4} Å/°C for a and c respectively, as determined in this study. Different values were reported by JOHNSON and ANDREWS. It is at least qualitatively clear, however, that low cristobalite has large coefficients of thermal expansion in comparison to high cristobalite. It is of interest to examine the mechanism of expansion, particularly since the structures are simple in comparison with those of other silicates in general, and tektosilicates in particular. Expansion is controlled by two independent variables as described, for example, by FOREMAN and PEACOR (1970) for nepheline, and TAYLOR (1972) for framework silicates. First, the average cell volume can increase through a lengthening of mean bond distances. Secondly, expansion can occur through change in relative orientation of adjacent tetrahedra, with no change in geometry of the tetrahedron.

It is not possible to quantitatively and accurately assess the role played by change in bond distance as a function of temperature at this time, for several reasons. First, the distances between atoms as usually calculated are distances between mean positions uncorrected for thermal motion. Secondly, available models for corrections for thermal motion are approximations which require prior assessment of the mode of interaction of adjacent atoms, and except for structures with discrete molecules, have questionable meaning. In addition, the thermal-vibration values are approximations to the actual systems, and assume harmonic vibration. However, the decreases in Si—O distances with increasing temperature, as shown in Fig. 6, represent a limiting case with no corrections for thermal motion. Corrections for thermal motion would increase these distances, but to an unpredictable degree. The mean distances may actually increase slightly, remain constant, or show a smaller rate of increase than represented in Fig. 6.

In high cristobalite there is negligible thermal expansion. The only contributing variable structure parameters, since the positions of the Si atoms are fixed, are change in the Si—O distance (with a concomitant change in the Si—Si distance), and change in the Si—O—Si angle. As noted above, these parameters (as determined using mean atom positions) are strongly dependent. As the apparent value of Si—O decreases, the Si—O—Si angle increases, with increasing temperature. Each of these has an opposite and compensating effect on the Si—Si separation. The decrease in Si—O and the increase in Si—O—Si, as determined using mean atom positions, thus qualitatively accounts for the low thermal-expansion coefficient in high cristobalite.

In low cristobalite, on the other hand, the positions of both Si and O are not fixed by symmetry, and change regularly toward those of high cristobalite with increasing temperature, as shown in a preceding section. As a result of changing relative orientation of tetrahedra, as partially reflected in the Si—O—Si angles of Table 4, both *a* and *c* must increase, independently of change in tetrahedron geometry. This effect is the principal cause of the moderately high thermal-expansion coefficients in low cristobalite. It is interesting to note that the geometry of the tetrahedra, as reflected in the O—Si—O angles of Table 4, is virtually constant over all temperatures, within standard error. At least in this case, temperature has almost no effect on the tetrahedron geometry, with the exception of the apparent minor changes in Si—O distances. The principal structural change is in the relative orientations of the tetrahedra, as partially reflected in the apparent Si—O—Si angles.

Acknowledgement

Dr. CLIFFORD FRONDEL kindly made available a large number of the cristobalite crystals, and Dr. WAYNE DOLLASE also donated specimens. This work was supported by NSF Grant GA-17402 from the National Science Foundation.

References

TOM F. W. BARTH (1932a), The cristobalite structures: I. High cristobalite. Amer. Jour. Sci. **23**, 350—356.

TOM F. W. BARTH (1932b), The cristobalite structures: II. Low cristobalite. Amer. Jour. Sci. **24**, 97—110.

D. W. J. CRUICKSHANK (1965), Errors in least-squares methods. Chapter in *Computing methods in crystallography*, edited by J. S. ROLLET, Pergamon Press, Oxford.

W. A. DOLLASE (1965), Reinvestigation of the structure of low cristobalite. Z. Kristallogr. **121**, 369—377.

F. F. FOIT and D. R. PEACOR (1967), A high-temperature furnace for a single crystal x-ray diffractometer. J. Sci. Instrum. **44**, 183—185.

NEIL FOREMAN and D. R. PEACOR (1970), Refinement of the nepheline structure at several temperatures. Z. Kristallogr. **132**, 45—70.

W. JOHNSON and K. W. ANDREWS (1956), An x-ray study of the inversion and thermal expansion of cristobalite. Brit. Ceram. Soc. Trans. **55**, 227—235.

W. NIEUWENKAMP (1935), Die Kristallstruktur des Tief-Cristobalits SiO_2. Z. Kristallogr. **92**, 82—88.

W. NIEUWENKAMP (1937), Über die Struktur von Hoch-Cristobalit. Z. Kristallogr. **96**, 454—458.

DONALD R. PEACOR (1968), A high temperature single crystal diffractometer study of leucite, $(K,Na)AlSi_2O_6$. Z. Kristallogr. **127**, 213—224.

ROBERT B. SOSMAN (1965), *The phases of silica.* Quinn, Boden & Co., Rahway, New Jersey.

D. TAYLOR (1972), The thermal expansion behavior of the framework silicates. Mineral. Mag. **38**, 593—604.

A. VAN VALKENBURG, JR. and B. F. BUIE (1945), Octahedral cristobalite with quartz paramorphs from Ellora caves, Hyderabad State, India. Amer. Mineral. **30**, 526—535.

C. W. WOLFE (1945), Crystallography of cristobalite from Ellora caves, India. Amer. Mineral. **30**, 536—537.

M. J. WYART (1938), Etude sur la leucite. Bull. Soc. franç. Mineral. **61**, 228—238.

W. L. WYCKOFF (1925), The crystal structure of the high temperature form of cristobalite (SiO_2). Amer. Jour. Sci. **9**, 448—459.

R. A. YOUNG (1962), Mechanism of the phase transition in quartz. Final report to Air Force Office of Scientific Research, Project A-447.